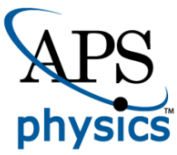

Galactic Center Excess in γ Rays from Annihilation of Self-Interacting Dark Matter

Manoj Kaplinghat, Tim Linden, and Hai-Bo Yu

Phys. Rev. Lett. **114**, 211303 — Published 27 May 2015

DOI: 10.1103/PhysRevLett.114.211303

Galactic Center Excess in Gamma Rays from Annihilation of Self-Interacting Dark Matter

Manoj Kaplinghat
Department of Physics and Astronomy, University of California, Irvine, CA 92697, USA

Tim Linden
Kavli Institute for Cosmological Physics, University of Chicago, IL 60637, USA

Hai-Bo Yu
Department of Physics and Astronomy, University of California, Riverside, CA 92521, USA

Observations by the Fermi-LAT telescope have uncovered a significant γ-ray excess directed toward the Milky Way Galactic Center. There has been no detection of a similar signal in the stacked population of Milky Way dwarf spheroidal galaxies. Additionally, astronomical observations indicate that dwarf galaxies and other faint galaxies are less dense than predicted by the simplest cold dark matter models. We show that a self-interacting dark matter model with a particle mass of roughly 50 GeV annihilating to the mediator responsible for the strong self-interaction can simultaneously explain all three observations. The mediator is necessarily unstable and its mass must be below about 100 MeV in order to decrease the dark matter density of faint galaxies. If the mediator decays to electron-positron pairs with a cross section on the order of the thermal relic value, then we find that these pairs can up-scatter the interstellar radiation field in the Galactic Center and produce the observed γ-ray excess.

The Galactic Center excess. Recent Fermi-LAT observations of the Galactic Center (GC) of the Milky Way have uncovered a stunning γ-ray excess compared to expectations from diffuse astrophysical emission [1–11]. While these studies employ different astrophysical background models, they agree on three key features of the γ-ray excess: (1) the spectrum is strongly peaked at an energy of approximately 2 GeV, with a low-energy spectrum that is harder than expected from π^0-emission, (2) the excess radially extends to at least 10° from the GC, following an emission profile that falls with distance (r) from the GC as $r^{-\alpha}$ with $\alpha = 2.0 - 2.8$, and (3) the excess is roughly spherically symmetric, without any evidence of elongation parallel or perpendicular to the galactic plane.

While other explanations have been discussed [4, 5, 12–15], dark matter remains a compelling possibility. The detection of an equivalent excess in the population of dwarf spheroidal galaxies surrounding the Milky Way would verify this possibility. However, no equivalent signal has been observed in dwarf spheroidal galaxies [16], which stands in mild tension with some models of the GC excess [17].

In fact, dwarf galaxies have long challenged our understanding of the nature of dark matter. The dark matter halos of dwarf galaxies have constant density cores [18–22], in contrast to the cuspy profile predicted by simulations of cold collisionless dark matter (CDM). Additionally, CDM predicts a population of dwarf halos that are systematically denser than the dwarf spheroidal galaxies in the Milky Way [23], Andromeda [24], or Local Group [25, 26]. A compelling solution to these challenges is to assume that dark matter strongly interacts with itself [27, 28]. Recent simulations have shown that nuclear-scale dark matter self-interaction cross sections can produce heat transfer from the hot outer region to the cold inner region of dark matter halos, reducing the central densities of dwarf galaxies in accordance with observations [29–32].

Connection to dark matter self-interactions. We explore the intriguing possibility that the GC $\gamma-$ray excess is caused by the inverse Compton (IC) scattering of energetic e^+e^- from dark matter annihilation, and the absence of the GeV γ-ray signal in dwarf spheroids is a natural consequence of self-interacting dark matter (SIDM) models. Our key observations are as follows:

- Energetic e^+e^- from dark matter annihilation can effectively produce γ-rays in the GC through IC and bremsstrahlung, due to the high interstellar radiation field (ISRF) and gas densities in this region. The IC emission can explain the peak of the GC signal (at 2-3 GeV) for dark matter masses of approximately 20-60 GeV. The crucial requirement is the presence of a new source of e^+e^- with energies larger than 20 GeV, which produce γ-rays with peak energy of $\sim (20\ \mathrm{GeV}/m_e)^2 E_{\rm ISRF}$, assuming a typical ISRF photon energy $E_{\rm ISRF} \sim 1$ eV.
- The AMS-02 constraint [33] demands a softer electron spectrum than direct annihilation to e^+e^- and hence annihilation through a light mediator is a natural solution[1].
- A nuclear-scale dark matter self-scattering cross section requires a dark force carrier with a mass below ~ 100 MeV [34–36]. Annihilations through this

[1] Another possibility, which we do not explore here, is direct annihilation to $\mu^+\mu^-$, with e and τ channels suppressed.

mediator can kinematically couple only to e^+e^- and neutrinos in the standard model sector.

- The e^+e^- produced via dark matter annihilation do not produce appreciable γ-rays from dwarf galaxies due to their low starlight and gas densities.

- The SIDM density profile in the central region of the Milky Way is determined by the bulge potential [37]. Models of the galactic bulge imply that the dark matter density increases to within 1-2° from the GC and the annihilation power is significantly enhanced compared to the predictions of SIDM-only simulations.

A hidden sector dark matter model. We consider a simple hidden sector model in a dark matter particle, χ, couples to a vector mediator, ϕ, as $g_\chi \bar{\chi}\gamma_\mu\chi\phi^\mu$. To illustrate our main points, we take $m_\chi = 50$ GeV but note that m_χ is sensitive to the electron energy losses in the GC as well as the tail of the γ-ray excess spectrum and is uncertain by at least 50%. The relic density in this model is set by the annihilation process $\bar{\chi}\chi \to \phi\phi$ with a cross section $4.4\xi\times10^{-26}$ cm^{3}s^{-1} for a Dirac particle [38], where ξ is the ratio of the temperature of the hidden sector to that of the visible sector at freeze-out [39, 40]. This implies that $\alpha_\chi = g_\chi^2/4\pi \simeq 3.5\times10^{-5}(m_\chi/\mathrm{GeV})\sqrt{\xi}$.

In the halo, Sommerfeld enhancement at low velocities will increase the annihilation cross section by a factor $\bar{S}$ [41], which depends on $\alpha_\chi, m_\chi, m_\phi$ after averaging over the velocity distribution. Thus, the annihilation cross section relevant in the halo is $4.4\xi\bar{S}\times10^{-26}$ cm^{3}s^{-1}, where we have neglected the $\mathcal{O}(1)$ changes due to Sommerfeld enhancement at freeze-out [46].

ξ depends on the reheating temperatures of the dark and visible sectors as well as the entropy production between reheating and freeze-out [39]. For concreteness, we assume $\xi = 0.2$, which results in an effective enhacement for annihilation in the solar neighborhood $\xi\bar{S} \simeq 1$, assuming a dark matter velocity dispersion $\sigma_r = 150$ km/s (consistent with the halo model described later). The values chosen above are meant to be illustrative; many other solutions are possible, *e.g.*, for $m_\chi = 20$ GeV, the effective enhancement is about unity for $\xi = 0.5$.

The mediator has to be unstable otherwise it will overclose the universe. We assume that the hidden and visible sectors are coupled through kinetic [42] or Z-mixing [43] leading to $\phi \to e^+e^-$ decays [44]. If the mediator decays before Big Bang Nucleosynthesis (BBN), then the model is guaranteed to pass all cosmological tests. This requirement puts a lower bound on the mixing parameter, while the direct detection experiments put an upper bound on this mixing parameter. For both kinetic mixing and Z-mixing, a mixing parameter around 10^{-10} satisfies BBN and direct detection constraints [44] and is safe from flavor constraints [45]. With such a small mixing parameter, the two sectors will not thermalize in the early universe [46, 47] and thus $\xi \neq 1$ naturally. In addition, the mediator lifetime of ~ 1 sec is short enough that we can assume the mediator decays instantly when produced in the GC.

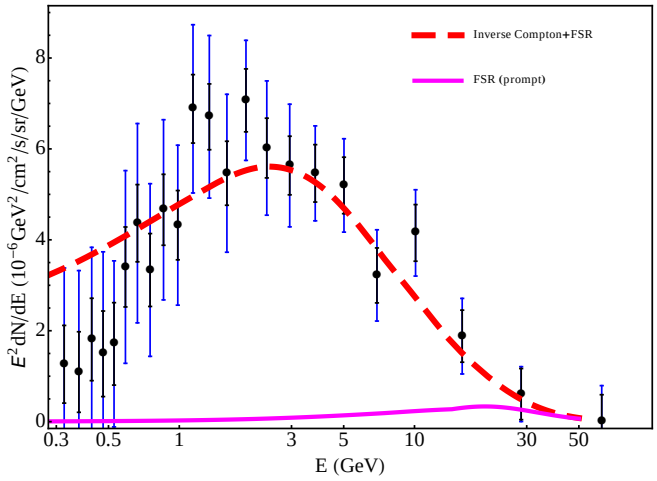

FIG. 1. γ-ray spectrum from Inverse Compton emission and final state radiation produced by annihilation of a 50 GeV dark matter particle through a light mediator into e^+e^- final state. The spectrum is compared to the Galactic Center excess [10].

In order to compute the secondary emission from this model we utilize the software `PPPC4DMID` [48], which provides the solution for one-dimensional diffusion with spatially dependent energy losses. We use the "MED" diffusion parameters listed in `PPPC4DMID` [48]. This software calculates the γ-ray spectrum from IC scattering assuming an interstellar radiation field energy density from `GALPROP` [49], an exponential magnetic field profile [50], and negligible bremsstrahlung losses. These approximations are valid for the $\gtrsim 10$ GeV electrons under consideration. We tested the `PPPC4DMID` spectrum by writing an independent code that solves the one-dimensional diffusion equation assuming spatially-constant energy losses and found good agreement.

In Fig. 1, we show that the intensity and spectrum of our model provides a good fit to the analysis of the GC excess produced by Ref. [10]. Specifically, we compare our results to their ROI I, which includes regions within 5° radius (about 750 pc projected distance at the GC) excluding latitudes $|b| < 2°$. These results show that the secondary IC emission effectively reproduces the hard spectral bump at an energy of $\sim$2 GeV, and the relatively hard spectrum component at energies above 10 GeV observed by Ref. [10]. The hard spectrum component is an important discriminator of the dark matter mass, as it is absent for lower masses $\sim$20 GeV.

We estimate the range of cross sections required to produce this signal as $0.3-2\times10^{-26}$cm^3/s, corresponding to the SIDM density profiles shown in Fig. 2 and discussed below. In order to estimate this cross section range we noted (using the density profiles available in `PPPC4DMID`) that the IC signal (shown in Fig. 3) is proportional to the J-factor ($J = \int d\ell\rho^2(\ell,\Omega)$, where ℓ = line of sight)

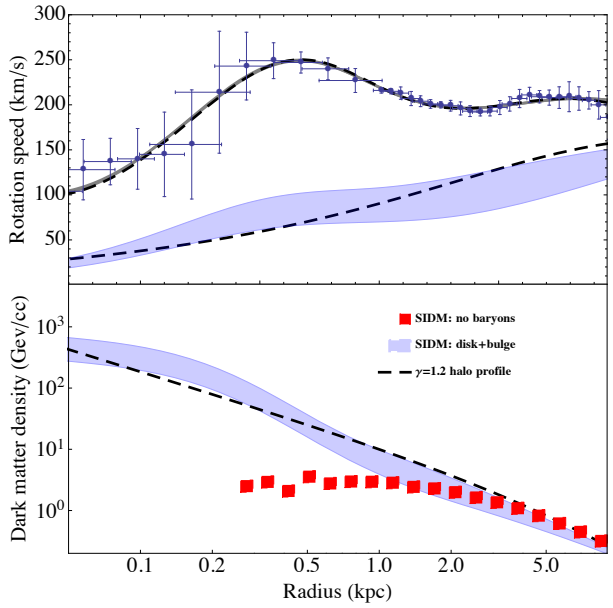

FIG. 2. The top panel shows the rotation curve data for the Milky Way complied by Ref. [54] and fits described in the text. In the panel below, the adopted $\gamma = 1.2$ density profile (dashed) is compared to SIDM predictions (shaded), with the filled points showing the density profile predicted for SIDM without including baryons [30].

within 5 degrees of the GC at the 10% accuracy level. Therefore, we scale the `PPPC4DMID` result using the J-factors for the SIDM density profiles to obtain the cross section range.

Density profile of SIDM. The calculation of the annihilation cross-section depends on the dark matter density profile. SIDM-only simulations generally predict that the dark matter density profile would be essentially constant near the GC. However, when baryons dominate, as expected in the inner galaxy, it has been shown that the equilibrium SIDM density profile tracks the baryonic potential [37]. We compute the equilibrium SIDM density profile assuming two possibilities for the initial (before self-interactions become effective) dark matter density profile following the method in Ref. [37]: an NFW profile [51] with scale factor $r_s = 26$ kpc [52] and the same profile after adiabatic contraction [53] due to the disk and bulge of the Milky Way. These profiles set the boundary conditions for the equilibrium solutions.

We determine the consistency of this scenario by fitting to the composite galactic rotation curve of Ref. [54] shown in the top panel of Fig. 2 including a black hole of mass $4 \times 10^6 M_\odot$, inner and outer spherical bulges with exponential density profiles, an exponential disk and a spherical halo. The SIDM halo is computed self-consistently from the spherically-averaged stellar distribution. The general non-spherical equilibrium solution [37, 55] would require non-spherical modeling of the bulge, which is beyond the scope of this work.

A simple iterative procedure suffices to find the best fit values after varying the outer bulge and disk parameters. The inner bulge and black hole mass are not varied as the SIDM halo profile outside 100 pc is less sensitive to them. The SIDM halo has two free parameters: a central density (ρ_0) and central velocity dispersion (σ_0). We fix $\sigma_0 = 170$ km/s and vary ρ_0 as described above. Equilibrium solutions also exist for slightly different values of σ_0, but do not affect our key results.

The SIDM fits and the density profiles are shown in Fig. 2, with the edges of the shaded band arising from the two assumptions about the early dark matter profile. For comparison, we also show the fit to the composite rotation curve with an NFW-like dark matter profile $\rho \propto r^{-\gamma}(1 + r/r_s)^{\gamma-3}$ with $\gamma = 1.2$, $r_s = 10$ kpc and local density of 0.3 GeV/cm^3. We choose this profile since $\gamma = 1.2$ is consistent with the GC excess fits [6–8, 10] and it also closely tracks the adiabatically contracted profile mentioned previously.

Our bulge parameters are consistent with Ref. [54]. The main bulge has an exponential scale radius of approximately 0.13 kpc and total mass of $8 - 9 \times 10^9 M_\odot$ depending on the model. The scale radius is significantly smaller than the bulge radius found in photometric studies of the bulge [56–58], perhaps due to additional bulge structures in the inner 0.3 kpc, for which there is indirect evidence [59]. For our purposes, the present model suffices to convert the observed rotation curve to a baryonic potential, which then determines the SIDM density profile.

The main point of this exercise is to emphasize that SIDM predicts high dark matter densities at the Milky Way center (and in other baryon-dominated galaxies) and to explicitly show that these dark matter densities are compatible with current rotation curve data. Thus, the SIDM annihilation J-factor is comparable to or larger than the CDM predictions.

Morphology of the excess. Unlike the case of the prompt signal, which is proportional to the annihilation power (density squared), the IC morphology is affected by diffusion and energy losses. In addition, different studies of the GC and inner galaxy [6–8, 10] have inferred somewhat different spatial templates for the signal. These facts suggest that signal morphology may be an important discriminant but more work is required.

We note that despite the interaction of the e^+e^- flux with the non-spherical ISRF, the resultant IC signal (using `PPPC4DMID`) is roughly spherically symmetric (to within 10% in the ROI), in agreement with present estimates [8]. Diffusion and energy losses may also moderate any asphericity in the annihilation power, suggesting that the sphericity of the GeV excess can be accommodated in this SIDM scenario.

In comparison, for a prompt signal to be spherical, one must appeal to significant gas cooling in the halo centers after all the major mergers [60] since CDM halos without baryons are highly aspherical in their centers [61]. However, adiabatic contraction due to this cooling may result in $\gamma \approx 2$ [62], which would be inconsistent with the

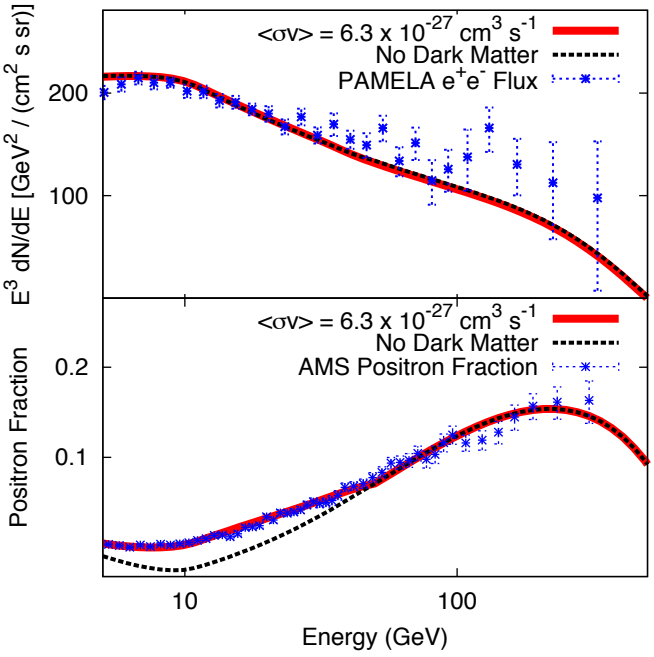

FIG. 3. The e^+e^- spectrum (top) and positron fraction (bottom) for the SIDM model, compared to observations from PAMELA and AMS-02, respectively. Note that excellent fits with no dark matter can be found by varying the diffusion and solar modulation parameters away from what has been assumed here.

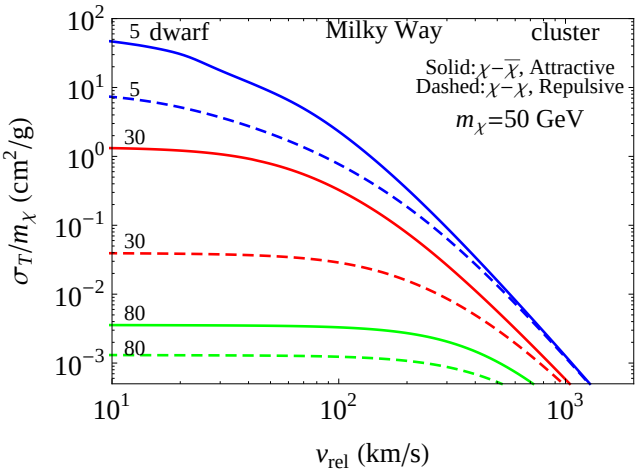

FIG. 4. Dark matter self-interaction cross section as a function of the dark matter relative velocity for mediator mass 5 MeV (Blue), 30 MeV (red), and 80 MeV (Green). SIDM models with $\sigma_T/m_\chi \sim 0.5-50$ cm^2/g on dwarf scales can produce constant density cores in dwarf galaxies in accordance with observations [32].

GeV excess templates. There seems to be no clear prediction for the morphology of prompt gamma-rays from dark matter annihilation.

AMS-02 constraint. The strongest constraint on SIDM models stems from observations of the local positron fraction by PAMELA [63] and AMS-02 [64]. To investigate this, we employ *Galprop* models [65] of the astrophysical electron and positron flux at Earth. We add a pulsar component modeled by a power-law injection of e^+e^- pairs with an exponential cutoff [66]. We add a dark matter annihilation component assuming the hidden and visible sectors are coupled through Z-boson mass mixing, with $\xi\bar{S} = 1$ and an annihilation cross section to e^+e^- of $4.4\xi\bar{S} \times 10^{-26}$ cm^{3}s$^{-1}/7 = 6.3 \times 10^{-27}$ cm^{3}s^{-1} [44]. This cross section is within the range computed previously to explain the GeV excess.

We use the $\gamma = 1.2$ profile for the dark matter with a local density of 0.3 GeV cm^{-3} shown in Fig. 2 since it tracks the upper edge of the shaded band near the solar location and results in a conservative AMS-02 constraint. We test an ensemble of diffusion parameters and find the model producing the best combined fit to the AMS-02 positron fraction and the PAMELA e^+e^- flux. The resulting diffusion parameters are not far from those calculated for cosmic-ray nuclei [67]. Specifically we use a diffusion constant of 9.1×10^{28} cm^{2}s^{-1}, a half-scale height of 6.6 kpc, an Alfvén velocity of 30.5 km s^{-1}, and a primary cosmic-ray electron spectrum following a broken power-law falling as $E^{-2.23}$ below 11.4 GeV and as $E^{-2.79}$ at higher energies. We adopt charge-dependent solar modulation, with amplitudes of $\phi_{e^+} = 171$ MV for positrons and $\phi_{e^-} = 54$ MV for electrons.

The result shown in Fig. 3 indicates that annihilations through a light mediator can reproduce the intensity of the GC excess while remaining consistent with AMS-02 constraints. We note that the formal fit for AMS-02 data is quite good (χ^2/d.o.f. = 1.32), but poor for PAMELA data (χ^2/d.o.f. = 3.07). However, we find this to be of a similar quality to fits produced without a dark matter component. Interestingly, updated measurements by AMS-02 offer the exciting possibility of constraining or detecting SIDM annihilation. We note that these findings are consistent with [33], given that we adopt a local density of 0.3 GeV cm^{-3}, as opposed to 0.4 GeV cm^{-3}, and noting that the annihilations through a light mediator soften the resulting e^+e^- injection spectrum, making it more comparable to annihilation through $\mu^+\mu^-$ than direct annihilation to e^+e^-.

SIDM solution to small-scale structure formation problems. In Fig. 4, we show the dark matter self-interaction cross section as a function of the dark matter relative velocity. For $m_\chi = 50$ GeV, we need $m_\phi \lesssim 30$ MeV for self-interactions to solve anomalies on dwarf scales. It is interesting to note that for attractive interactions σ_T is enhanced when the mediator mass is 5 MeV because of the s-wave resonance with n=2 [68]. The cross section σ_T drops slightly on Milky Way scales, but is still large enough to effect the Milky Way halo [37]. On cluster scales, dark matter self-scattering is highly suppressed as $1/v_{\rm rel}^4$, because the momentum transfer is much larger than the mediator mass and dark matter self-scattering occurs in the Rutherford scattering limit.

Therefore, the model is fully consistent with the Bullet Cluster [69] and cluster shape [70] constraints.

Other detectable features. In addition to producing a correlation between the density profile of dark matter and the galactic bulge, as well as producing a significant contribution to the AMS-02 positron fraction, the dark matter model described here may be tested through radio observations. Specifically, the large e^+e^- flux predicted by our model may be able to explain (or be constrained by) the Green Bank Telescope radio continuum observations towards the GC [71], the isotropic emission detected by ARCADE-2 [72–75] and the observation of hard-spectrum radio filaments in the GC [76]. The event energy spectrum in direct detection experiments will be different from that predicted for contact interactions because the mediator mass is comparable to the momentum transfer of nuclear recoils [44, 77], which could provide a smoking-gun signature for SIDM.

The effective Sommerfeld enhancement for annihilation can be large (few to 10 or even larger at resonance) in dwarf galaxies. This opens up the possibility of searching for the prompt γ-ray emission due to final state radiation, which has a much harder spectrum compared to the GeV excess (see Fig. 1). This motivates a reanalysis of the Fermi-LAT dwarf galaxy observations with the final state radiation spectrum.

Summary. We show that the GC excess can be explained through secondary emission from e^+e^- pairs produced in dark matter annihilation events, a scenario which naturally predicts suppressed γ-ray emission from dwarf spheroidal galaxies. This class of models is well-motivated in the context of SIDM models posited to explain anomalies in the dark matter density profiles of dwarf spheroidal galaxies and other baryon-poor galaxies. These models make unique predictions, which could be tested in the near future.

While this paper was in preparation, several related papers were submitted by other groups [78, 79]. We note that our favored SIDM mass range is consistent with the analysis of light-mediator models by [78].

Acknowledgements - We thank Francesca Calore for providing the data employed in Fig. 1. MK is supported by NSF Grant No. PHY-1214648. TL is supported by the National Aeronautics and Space Administration through Einstein Postdoctoral Fellowship Award Number PF3-140110. HBY is supported by startup funds from UCR. We thank the Aspen Center for Physics and the NSF Grant-1066293 for hospitality during the conception of this paper.

[1] L. Goodenough and D. Hooper, (2009), 0910.2998.
[2] D. Hooper and L. Goodenough, Phys.Lett. **B697**, 412 (2011), 1010.2752.
[3] D. Hooper and T. Linden, Phys.Rev. **D84**, 123005 (2011), 1110.0006.
[4] K. N. Abazajian and M. Kaplinghat, Phys.Rev. **D86**, 083511 (2012), 1207.6047.
[5] C. Gordon and O. Macias, Phys.Rev. **D88**, 083521 (2013), 1306.5725.
[6] O. Macias and C. Gordon, Phys.Rev. **D89**, 063515 (2014), 1312.6671.
[7] K. N. Abazajian, N. Canac, S. Horiuchi, and M. Kaplinghat, Phys.Rev. **D90**, 023526 (2014), 1402.4090.
[8] T. Daylan *et al.*, (2014), 1402.6703.
[9] B. Zhou *et al.*, (2014), 1406.6948.
[10] F. Calore, I. Cholis, and C. Weniger, (2014), 1409.0042.
[11] K. N. Abazajian, N. Canac, S. Horiuchi, M. Kaplinghat, and A. Kwa, (2014), 1410.6168.
[12] K. N. Abazajian, JCAP **1103**, 010 (2011), 1011.4275.
[13] J. Petrovic, P. D. Serpico, and G. Zaharijas, (2014), 1411.2980.
[14] E. Carlson and S. Profumo, Phys.Rev. **D90**, 023015 (2014), 1405.7685.
[15] J. Petrovic, P. D. Serpico, and G. Zaharijas, JCAP **1410**, 052 (2014), 1405.7928.
[16] A. Geringer-Sameth, S. M. Koushiappas, and M. G. Walker, (2014), 1410.2242.
[17] Fermi-LAT Collaboration, B. Anderson *et al.*, (2014), Presentation at 5th Fermi Symposium.
[18] B. Moore, Nature **370**, 629 (1994).
[19] R. A. Flores and J. R. Primack, Astrophys.J. **427**, L1 (1994), astro-ph/9402004.
[20] M. G. Walker and J. Penarrubia, Astrophys.J. **742**, 20 (2011), 1108.2404.
[21] R. Kuzio de Naray, S. S. McGaugh, and W. de Blok, Astrophys.J. **676**, 920 (2008), 0712.0860.
[22] F. Donato *et al.*, Mon.Not.Roy.Astron.Soc. **397**, 1169 (2009), 0904.4054.
[23] M. Boylan-Kolchin, J. S. Bullock, and M. Kaplinghat, Mon.Not.Roy.Astron.Soc. **422**, 1203 (2012), 1111.2048.
[24] E. J. Tollerud, M. Boylan-Kolchin, and J. S. Bullock, Mon.Not.Roy.Astron.Soc. **440**, 3511 (2014), 1403.6469.
[25] E. N. Kirby, J. S. Bullock, M. Boylan-Kolchin, M. Kaplinghat, and J. G. Cohen, Mon.Not.Roy.Astron.Soc. **439**, 1015 (2014), 1401.1208.
[26] S. Garrison-Kimmel, M. Boylan-Kolchin, J. S. Bullock, and E. N. Kirby, Mon.Not.Roy.Astron.Soc. **444**, 222 (2014), 1404.5313.
[27] D. N. Spergel and P. J. Steinhardt, Phys.Rev.Lett. **84**, 3760 (2000), astro-ph/9909386.
[28] C. Firmani, E. D'Onghia, V. Avila-Reese, G. Chincarini, and X. Hernandez, Mon.Not.Roy.Astron.Soc. **315**, L29 (2000), astro-ph/0002376.
[29] M. Vogelsberger, J. Zavala, and A. Loeb, Mon.Not.Roy.Astron.Soc. **423**, 3740 (2012), 1201.5892.
[30] M. Rocha *et al.*, Mon.Not.Roy.Astron.Soc. **430**, 81 (2013), 1208.3025.
[31] J. Zavala, M. Vogelsberger, and M. G. Walker, Monthly Notices of the Royal Astronomical Society: Letters **431**, L20 (2013), 1211.6426.
[32] O. D. Elbert *et al.*, (2014), 1412.1477.
[33] L. Bergstrom, T. Bringmann, I. Cholis, D. Hooper, and C. Weniger, Phys.Rev.Lett. **111**, 171101 (2013), 1306.3983.

[34] S. Tulin, H.-B. Yu, and K. M. Zurek, Phys.Rev. **D87**, 115007 (2013), 1302.3898.
[35] J. M. Cline, Z. Liu, G. Moore, and W. Xue, Phys.Rev. **D90**, 015023 (2014), 1312.3325.
[36] K. K. Boddy, J. L. Feng, M. Kaplinghat, and T. M. P. Tait, Phys.Rev. **D89**, 115017 (2014), 1402.3629.
[37] M. Kaplinghat, R. E. Keeley, T. Linden, and H.-B. Yu, Phys.Rev.Lett. **113**, 021302 (2014), 1311.6524.
[38] G. Steigman, B. Dasgupta, and J. F. Beacom, Phys.Rev. **D86**, 023506 (2012), 1204.3622.
[39] J. L. Feng, H. Tu, and H.-B. Yu, JCAP **0810**, 043 (2008), 0808.2318.
[40] J. L. Feng, M. Kaplinghat, H. Tu, and H.-B. Yu, JCAP **0907**, 004 (2009), 0905.3039.
[41] N. Arkani-Hamed, D. P. Finkbeiner, T. R. Slatyer, and N. Weiner, Phys.Rev. **D79**, 015014 (2009), 0810.0713.
[42] B. Holdom, Phys.Lett. **B166**, 196 (1986).
[43] K. Babu, C. F. Kolda, and J. March-Russell, Phys.Rev. **D54**, 4635 (1996), hep-ph/9603212.
[44] M. Kaplinghat, S. Tulin, and H.-B. Yu, Phys.Rev. **D89**, 035009 (2014), 1310.7945.
[45] M. J. Dolan, C. McCabe, F. Kahlhoefer, and K. Schmidt-Hoberg, (2014), 1412.5174.
[46] J. L. Feng, M. Kaplinghat, and H.-B. Yu, Phys.Rev. **D82**, 083525 (2010), 1005.4678.
[47] D. Hooper, N. Weiner, and W. Xue, Phys.Rev. **D86**, 056009 (2012), 1206.2929.
[48] M. Cirelli *et al.*, JCAP **1103**, 051 (2011), 1012.4515.
[49] A. E. Vladimirov *et al.*, Comput.Phys.Commun. **182**, 1156 (2011), 1008.3642.
[50] A. W. Strong, I. V. Moskalenko, and O. Reimer, Astrophys.J. **537**, 763 (2000), astro-ph/9811296.
[51] J. F. Navarro, C. S. Frenk, and S. D. White, Astrophys.J. **490**, 493 (1997), astro-ph/9611107.
[52] F. Prada, A. A. Klypin, A. J. Cuesta, J. E. Betancort-Rijo, and J. Primack, Mon.Not.Roy.Astron.Soc. **428**, 3018 (2012), 1104.5130.
[53] G. R. Blumenthal, S. Faber, R. Flores, and J. R. Primack, Astrophys.J. **301**, 27 (1986).
[54] Y. Sofue, Publ.Astron.Soc.Jap. **65**, 118 (2013), 1307.8241.
[55] N. Amorisco and G. Bertin, Astron.Astrophys. **519**, A47 (2010), 0912.3178.
[56] L. Cao, S. Mao, D. Nataf, N. J. Rattenbury, and A. Gould, **MNRAS**, , Volume 434, Issue 1, p.595 (2013), 1303.6430.
[57] C. Wegg and O. Gerhard, Mon.Not.Roy.Astron.Soc. **435**, 1874 (2013), 1308.0593.
[58] R. K. Saito *et al.*, Astron.J. **142**, 76 (2011), 1107.5360.
[59] O. Gonzalez *et al.*, Astron.Astrophys. **534**, L14 (2011), 1110.0925.
[60] S. Kazantzidis *et al.*, Astrophys.J. **611**, L73 (2004), astro-ph/0405189.
[61] B. Allgood *et al.*, Mon.Not.Roy.Astron.Soc. **367**, 1781 (2006), astro-ph/0508497.
[62] M. Zemp, O. Y. Gnedin, N. Y. Gnedin, and A. V. Kravtsov, Astrophys.J. **748**, 54 (2012), 1108.5384.
[63] PAMELA Collaboration, O. Adriani *et al.*, Nature **458**, 607 (2009), 0810.4995.
[64] AMS Collaboration, M. Aguilar *et al.*, Phys.Rev.Lett. **110**, 141102 (2013).
[65] A. Strong and I. Moskalenko, Astrophys.J. **509**, 212 (1998), astro-ph/9807150.
[66] S. Profumo, Central Eur.J.Phys. **10**, 1 (2011), 0812.4457.
[67] R. Trotta *et al.*, Astrophys.J. **729**, 106 (2011), 1011.0037.
[68] S. Tulin, H.-B. Yu, and K. M. Zurek, Phys.Rev.Lett. **110**, 111301 (2013), 1210.0900.
[69] S. W. Randall, M. Markevitch, D. Clowe, A. H. Gonzalez, and M. Bradac, Astrophys.J. **679**, 1173 (2008), 0704.0261.
[70] A. H. Peter, M. Rocha, J. S. Bullock, and M. Kaplinghat, (2012), 1208.3026.
[71] F. Yusef-Zadeh *et al.*, Astrophys.J. **762**, 33 (2013), 1206.6882.
[72] D. Fixsen *et al.*, (2009), 0901.0555.
[73] N. Fornengo, R. Lineros, M. Regis, and M. Taoso, Phys.Rev.Lett. **107**, 271302 (2011), 1108.0569.
[74] D. Hooper *et al.*, Phys.Rev. **D86**, 103003 (2012), 1203.3547.
[75] K. Fang and T. Linden, (2014), 1412.7545.
[76] T. Linden, D. Hooper, and F. Yusef-Zadeh, Astrophys.J. **741**, 95 (2011), 1106.5493.
[77] N. Fornengo, P. Panci, and M. Regis, Phys.Rev. **D84**, 115002 (2011), 1108.4661.
[78] F. Calore, I. Cholis, C. McCabe, and C. Weniger, (2014), 1411.4647.
[79] J. Liu, N. Weiner, and W. Xue, (2014), 1412.1485.